Supporting Information

Use of fluorogenic Al^{3+} - Quinolinyl-azo-naphtholato complex for the determination of F^- in aqueous medium by visible light excitation and application on ground water fluoride analysis

Chandana Sen, Sunanda Dey, Chiranjit Patra, Debashis Mallick, Chittaranjan Sinha*

Table of Contents

Sl. No.	Contents	Scheme/Fig./Table No.
1.	FTIR spectrum of HL in KBr disk.	**Fig. S1**
2.	FTIR spectrum of $[AlL_2]^+NO_3$ in KBr disk.	**Fig. S2**
3.	^{1}H-NMR spectrum of HL in $CDCl_3$.	**Fig. S3**
4.	^{1}H-NMR spectrum of $[AlL_2]^+$ complex in DMSO-d_6.	**Fig. S4**
5.	HRMS spectrum of the receptor HL.	**Fig. S5**
6.	HRMS spectrum of the $[AlL_2]^+$ complex.	**Fig. S6**
7.	Synthetic process of the complex $[AlL_2]^+NO_3$.	**Scheme S1**
8.	Probable mechanism of *azo-hydrazo* tautomerisation of the chemosensor HL in methanol.	**Scheme S2**
9.	Absorption spectra of HL and different metals.	**Fig. S7**
10.	Determination of binding constant of HL for Al^{3+} from fluorescent titration data.	**Fig. S8**
11.	Linear response curve of HL at 612 nm depending on the Al^{3+} concentration.	**Fig. S9**
12.	ESI-MS spectrum of in-situ generated $[AlL_2]^+$ Complex with F^- ion; inset: zooming image from mass 50-290.	**Fig. S10**
13.	Job's plot of the chemosensor HL for Al^{3+}.	**Fig. S11**
14.	Linear response curve of $[AlL_2]^+$ at 612 nm depending on the F^- concentration.	**Fig. S12**
15.	Calibration plot between emission intensity of $[AlL_2]^+$	**Fig. S13**

	(Reference) at 612 nm vs volume of F^- for the analysis of F^- contamination in drinking water of Raghunathpur-I and Purulia-I in West Bengal.	
16.	**S**ome important bond length and bond angles of HL	**Table S1**
17.	**S**ome important bond length and bond angles of $[AlL_2]^+$	**Table S2**
18.	Contour plots of some selected molecular orbitals of HL.	**Fig. S14**
19.	Contour plots of some selected molecular orbitals of $[AlL_2]^+$ complex.	**Fig. S15**
20.	MO composition of HL.	**Table S3**
21.	MO composition of $[AlL_2]^+$.	**Table S4**
22.	Vertical electronic transitions calculated by TDDFT/B3LYP/CPCM method for HL and $[AlL_2]^+$.	**Table S5**

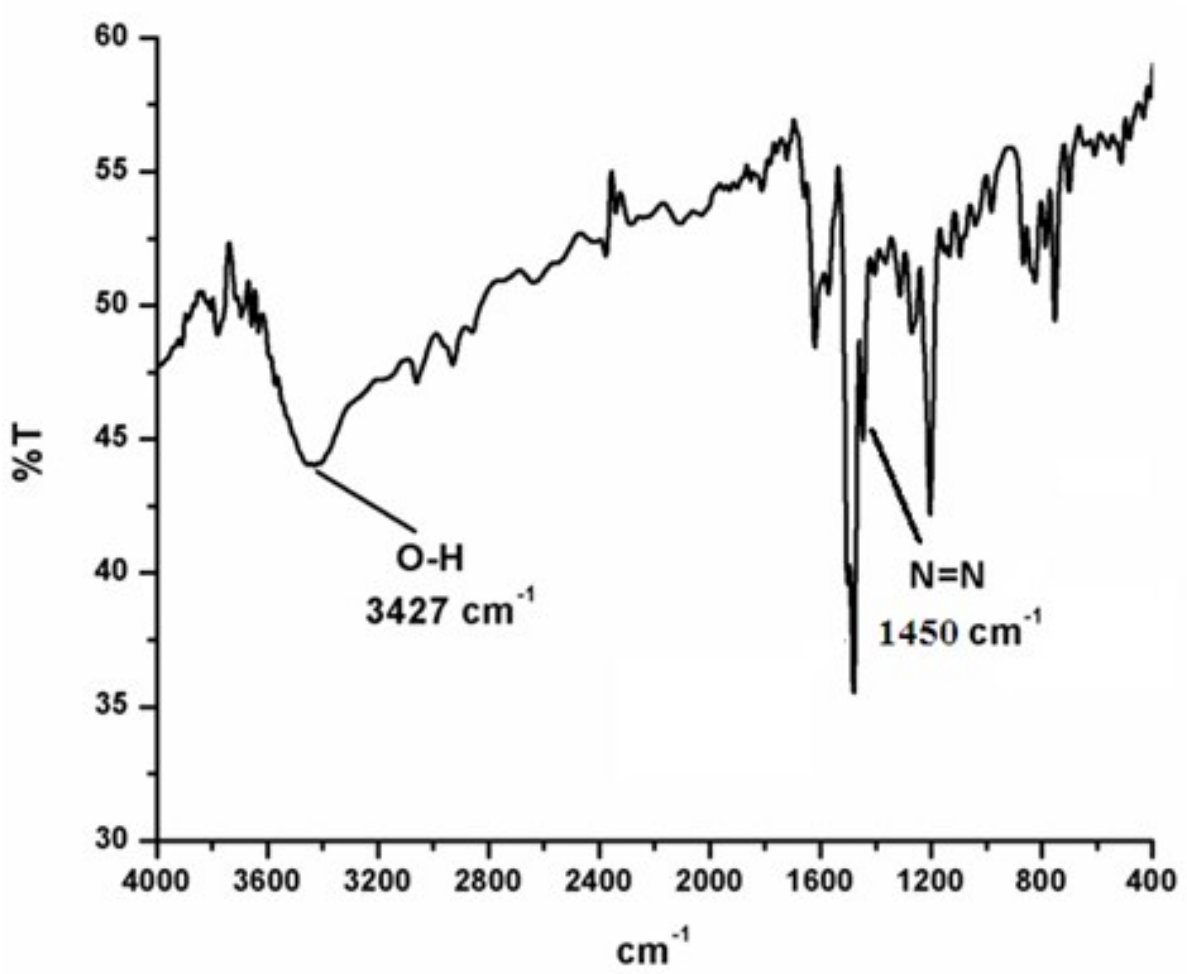

Fig. S1 FTIR spectrum of HL in KBr disk.

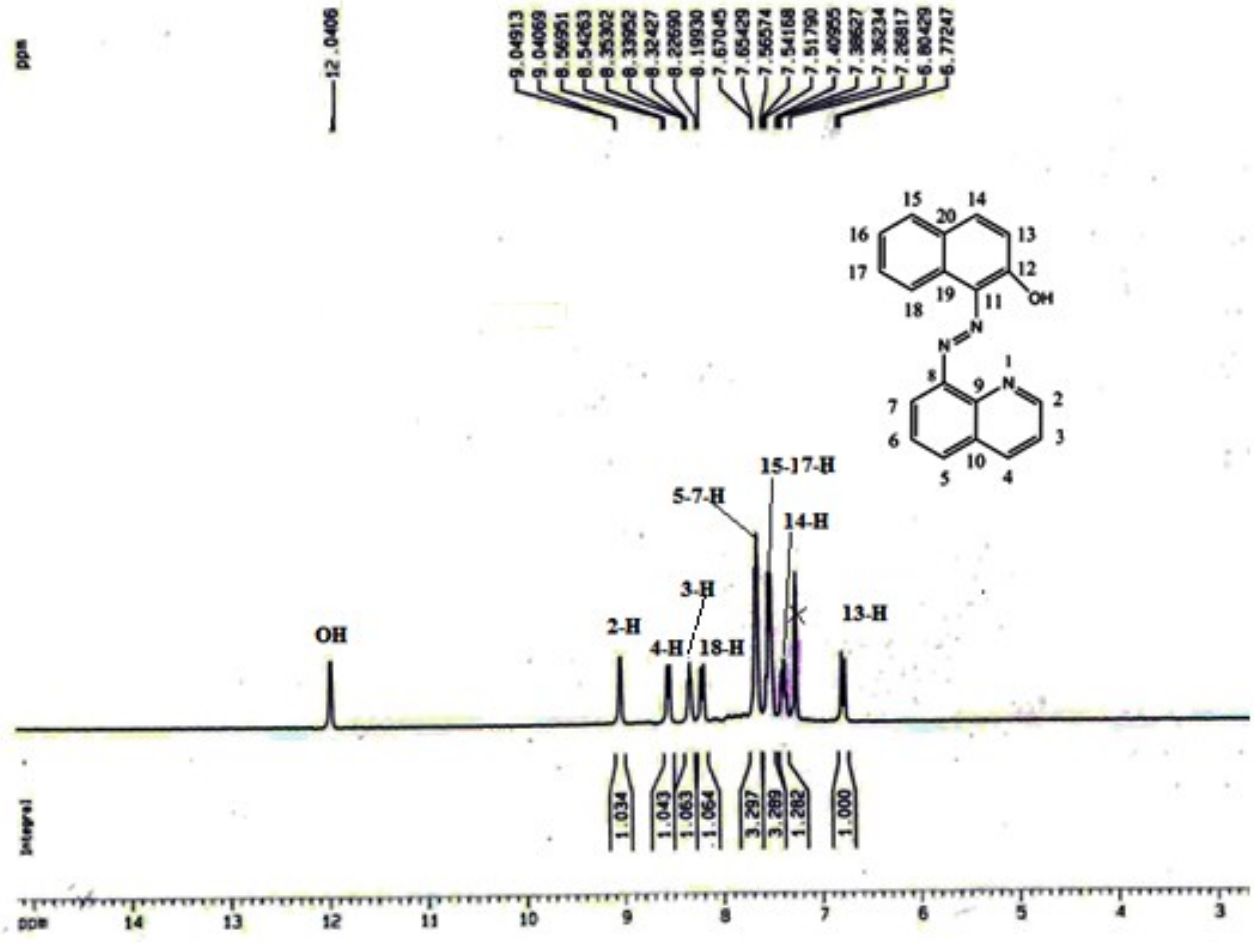

Fig. S2 ^{1}H-NMR Spectra of probe HL in $CDCl_3$.

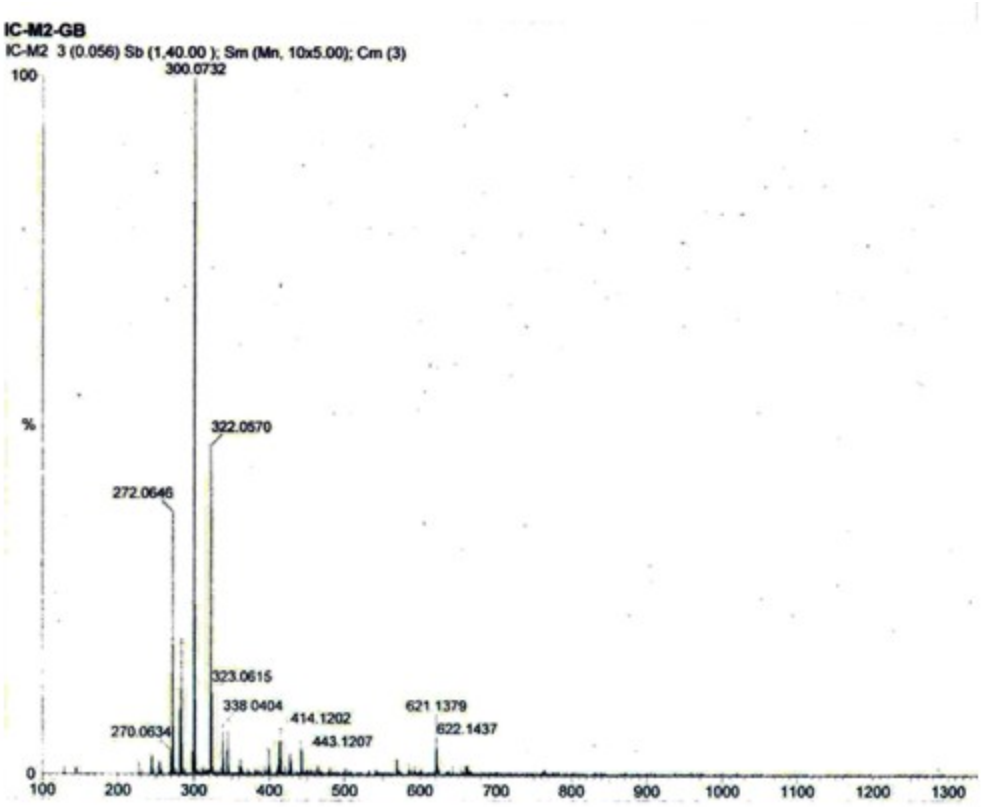

Fig. S3 Mass Spectrum of the probe HL.

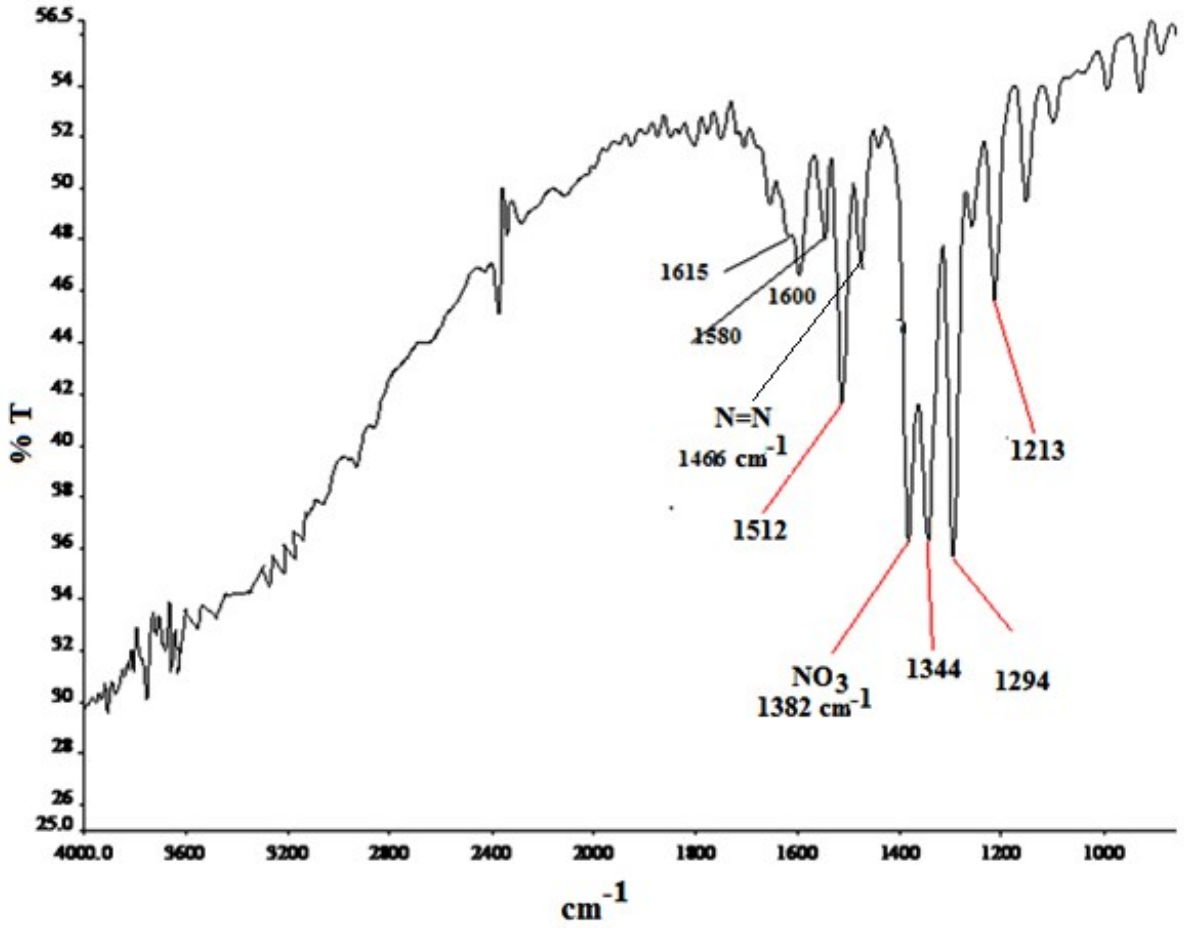

Fig. S4 FTIR spectrum of $[AlL_2]NO_3$ in KBr disk.

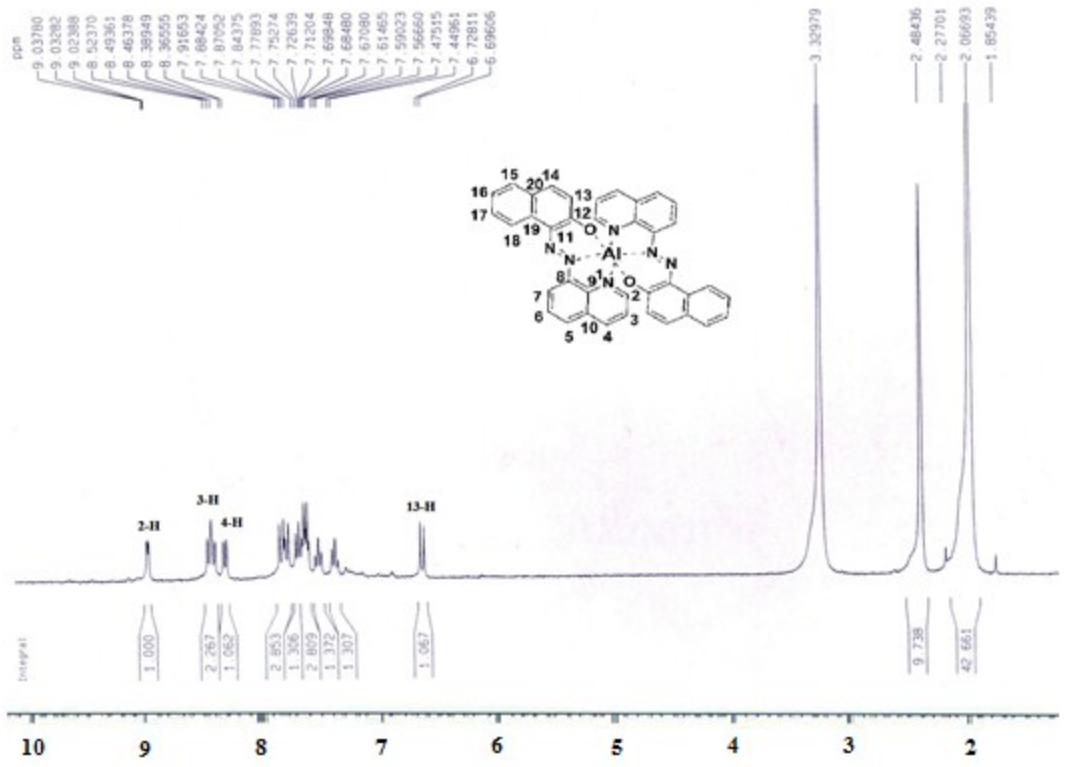

Fig. S5 ^{1}H-NMR Spectra of probe $[AlL_2]^+$ in DMSO-d_6.

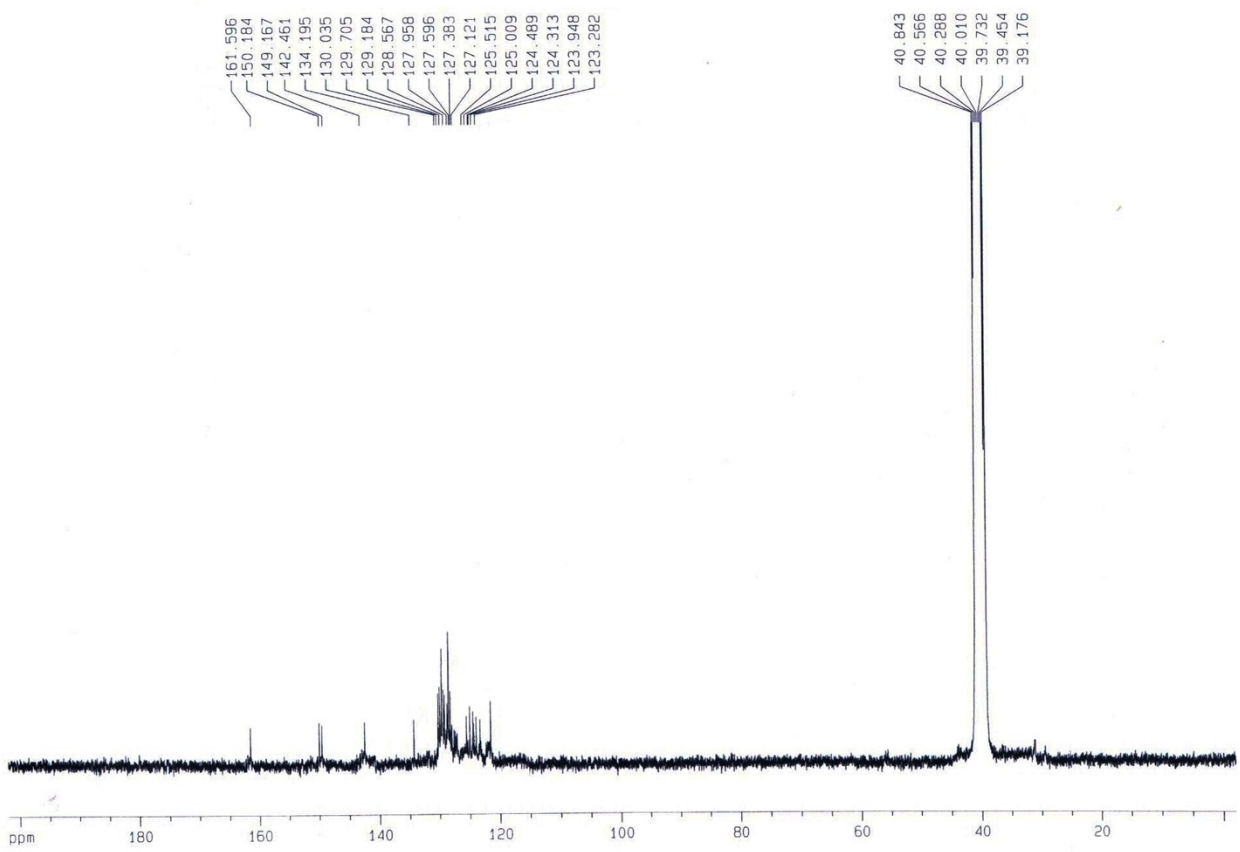

Fig. S6 ^{13}C NMR Spectrum of the $[AlL_2]^+$.

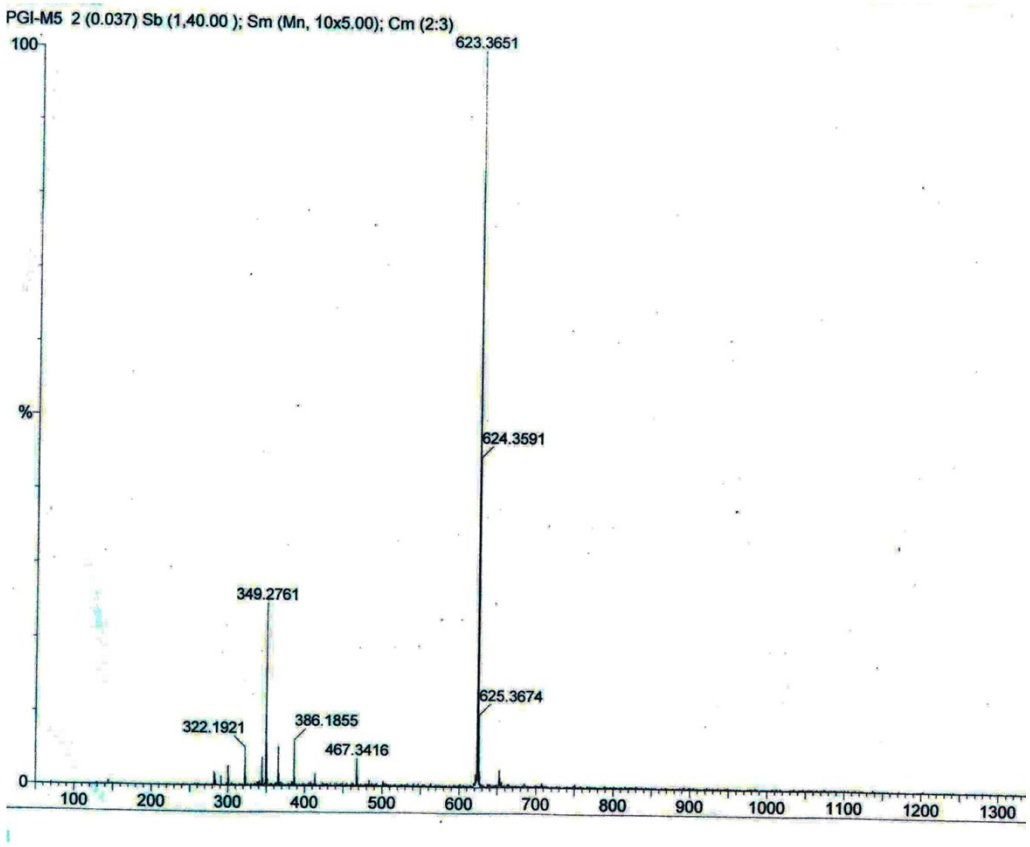

Fig. S7 Mass Spectrum of the $[AlL_2]^+$.

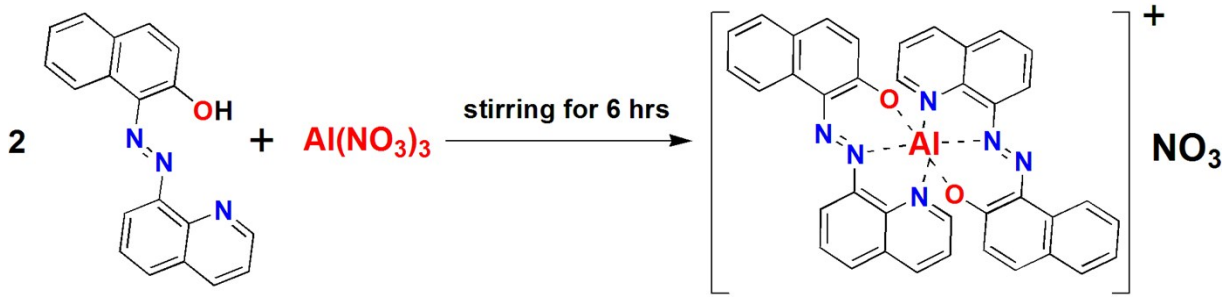

Scheme S1 Synthetic process of the complex $[AlL_2]NO_3$.

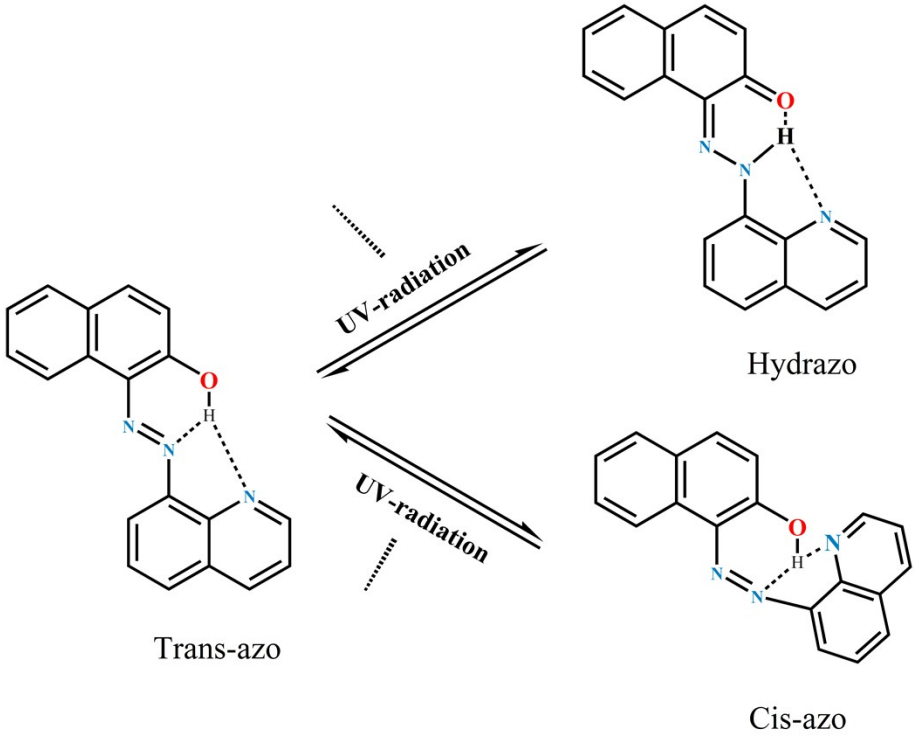

Scheme S2 Probable mechanism of *azo-hydrazo* tautomerisation of the chemosensor HL in methanol.

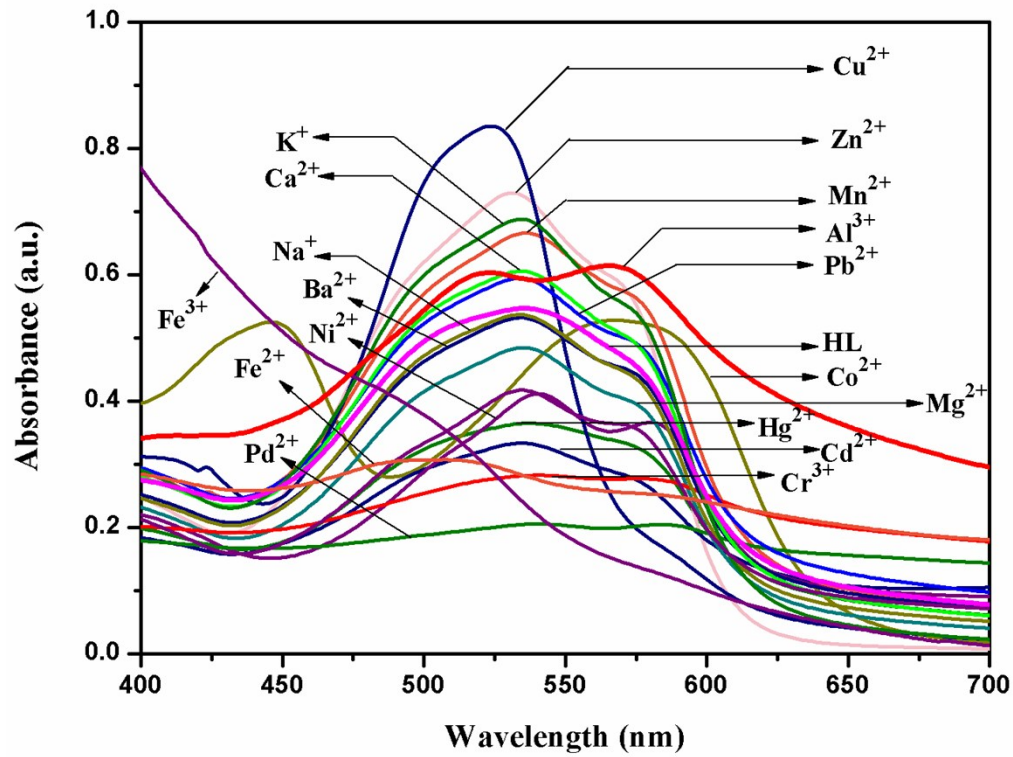

a

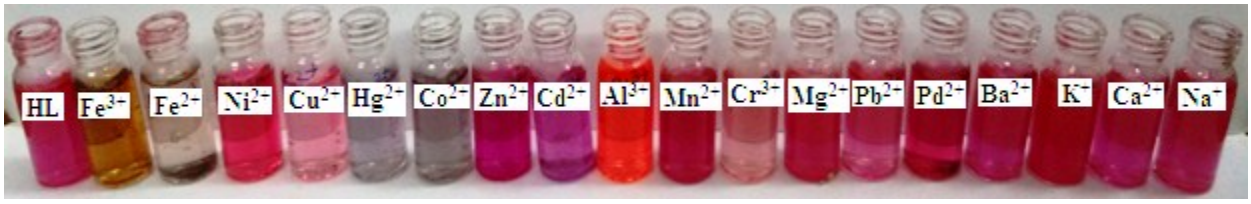

b

Fig. S8 (a) Absorption spectra of chemosensor (30 μM) in the presence of different metal ions (Ba^{2+}, Ca^{2+}, Co^{2+}, Cd^{2+}, Cr^{3+}, Cu^{2+}, Fe^{2+}, Fe^{3+}, Hg^{2+}, K^{+}, Na^{+}, Mg^{2+}, Mn^{2+}, Pb^{2+}, Zn^{2+}, Ni^{2+}, Pd^{2+} and Al^{3+}) (30 μM) in aqueous solution. (b) Vial images under visible light.

Binding constant was calculated according to the Benesi-Hildebrand equation. K_a was calculated following the equation stated below.

$$1/(F-F_o) = 1/\{K_a(F_{max}-F_o)\,[M^{n+}]^x\} + 1/[F_{max}-F_o]$$

Here F_0, F and F_{max} indicate the emission in absence of, at intermediate and at infinite concentration of metal ion respectively.

Plot of $[1/(F-F_0)]^2$ vs $1/[Al^{3+}]$ gives a straight line indicating 1:2 complexation between HL and Al^{3+} where K_a is found to be $2.54 \times 10^5\ M^{-1}$.

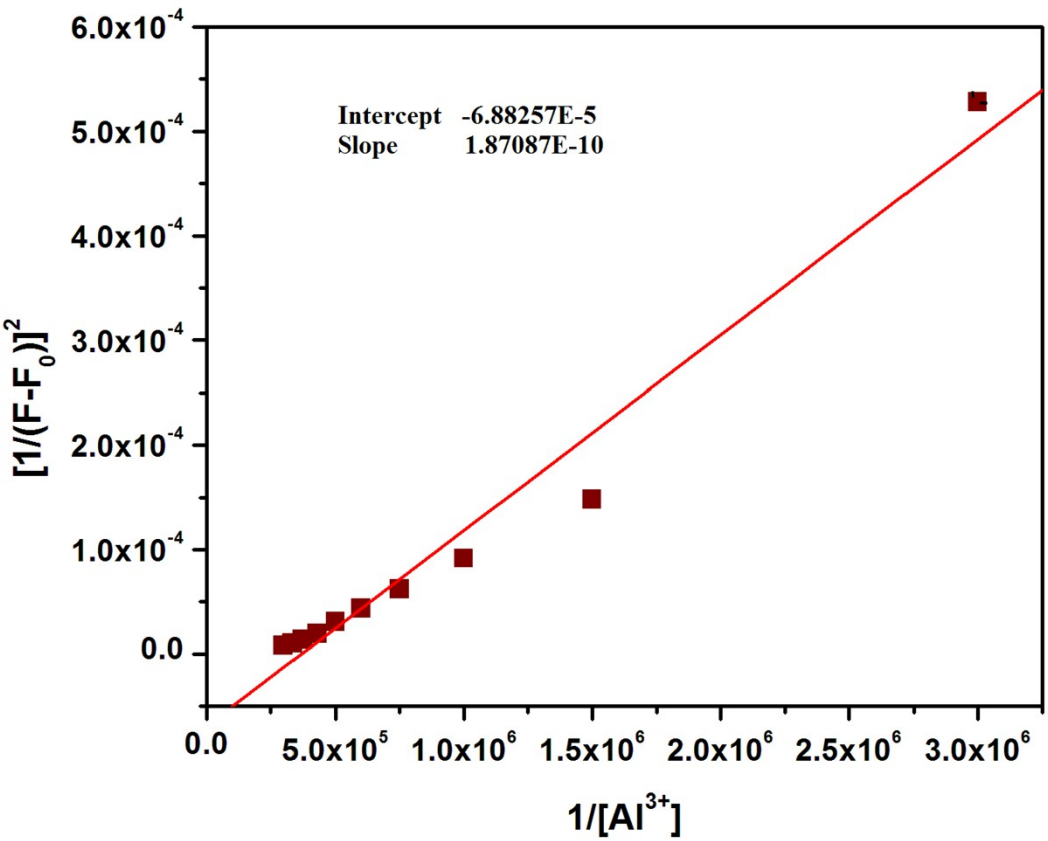

Fig. S9 Determination of binding constant of HL for Al^{3+} from fluorescent titration data.

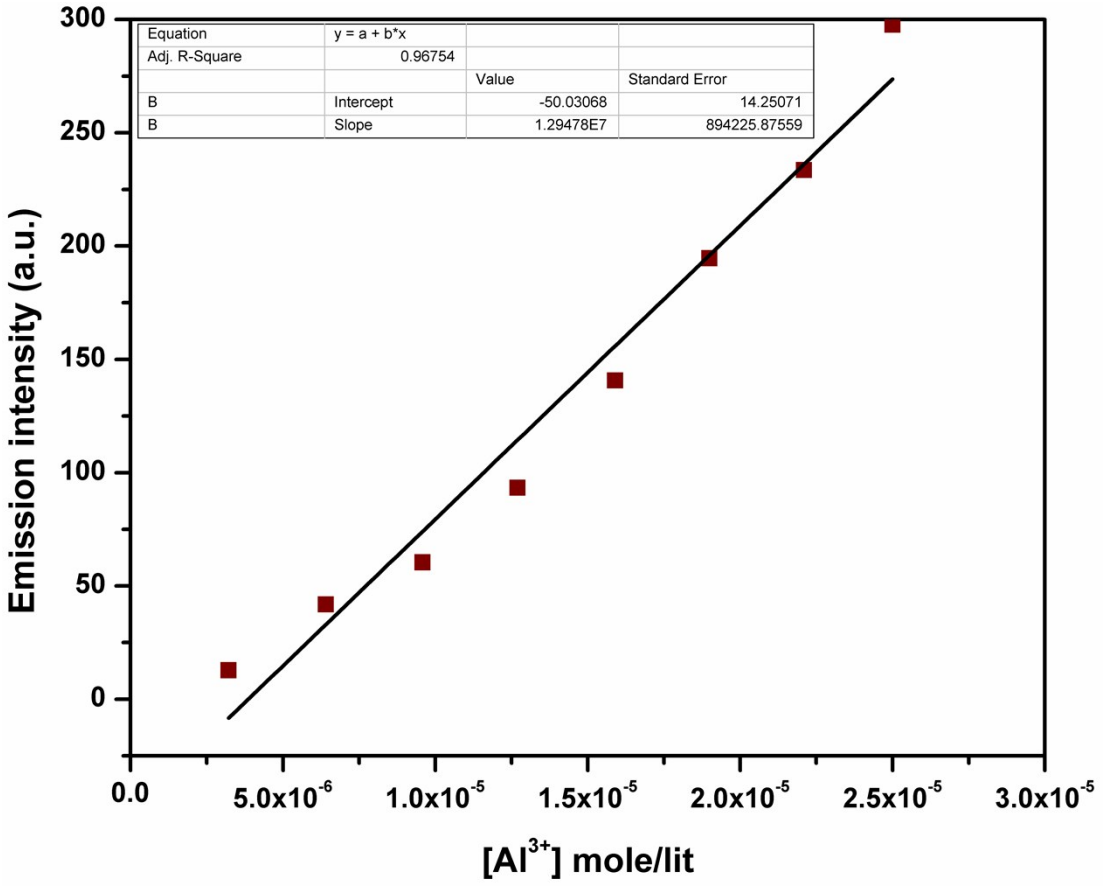

Fig. S10 Linear response curve of HL at 612 nm depending on the Al^{3+} concentration.

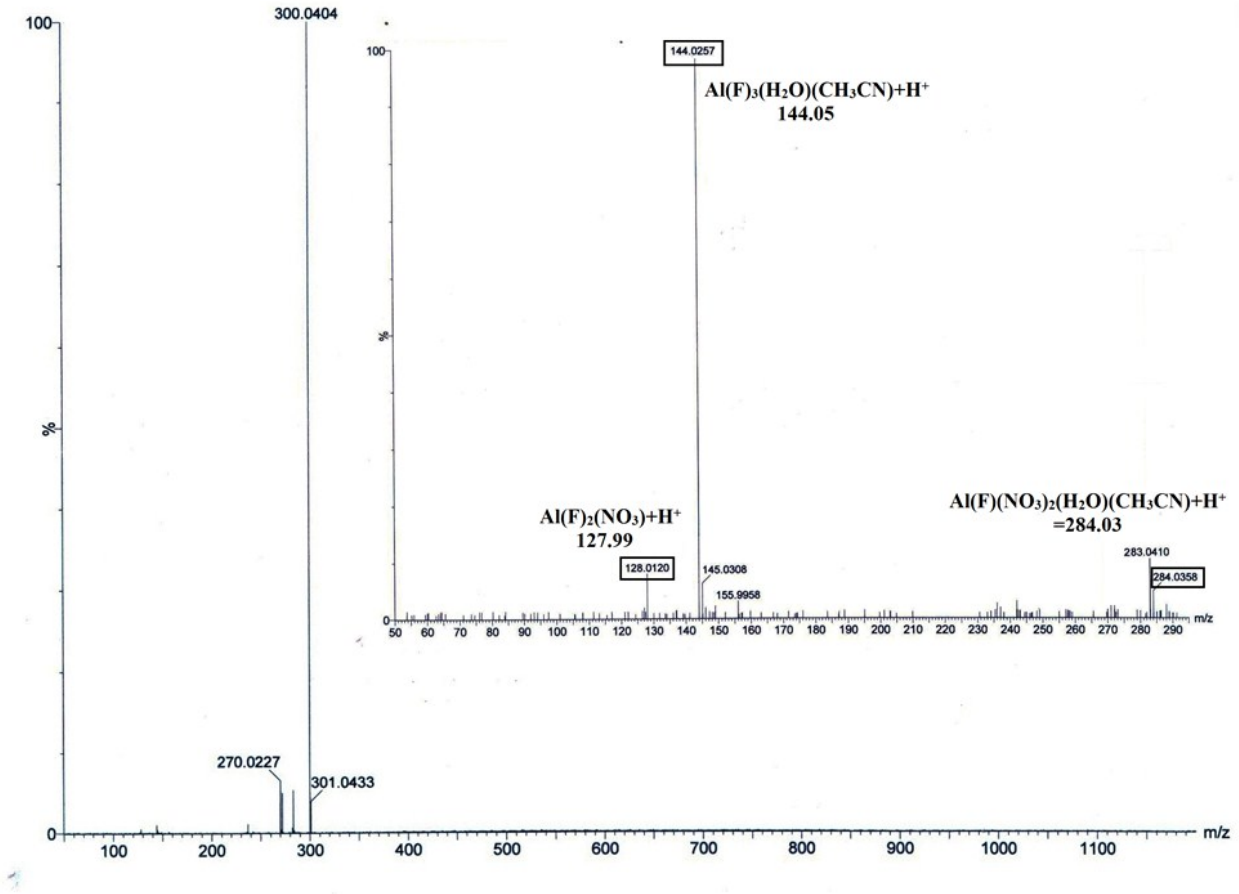

Fig. S11 ESI-MS spectrum of in-situ generated $[AlL_2]^+$ Complex with F^- ion; inset: zooming image from mass 50-290.

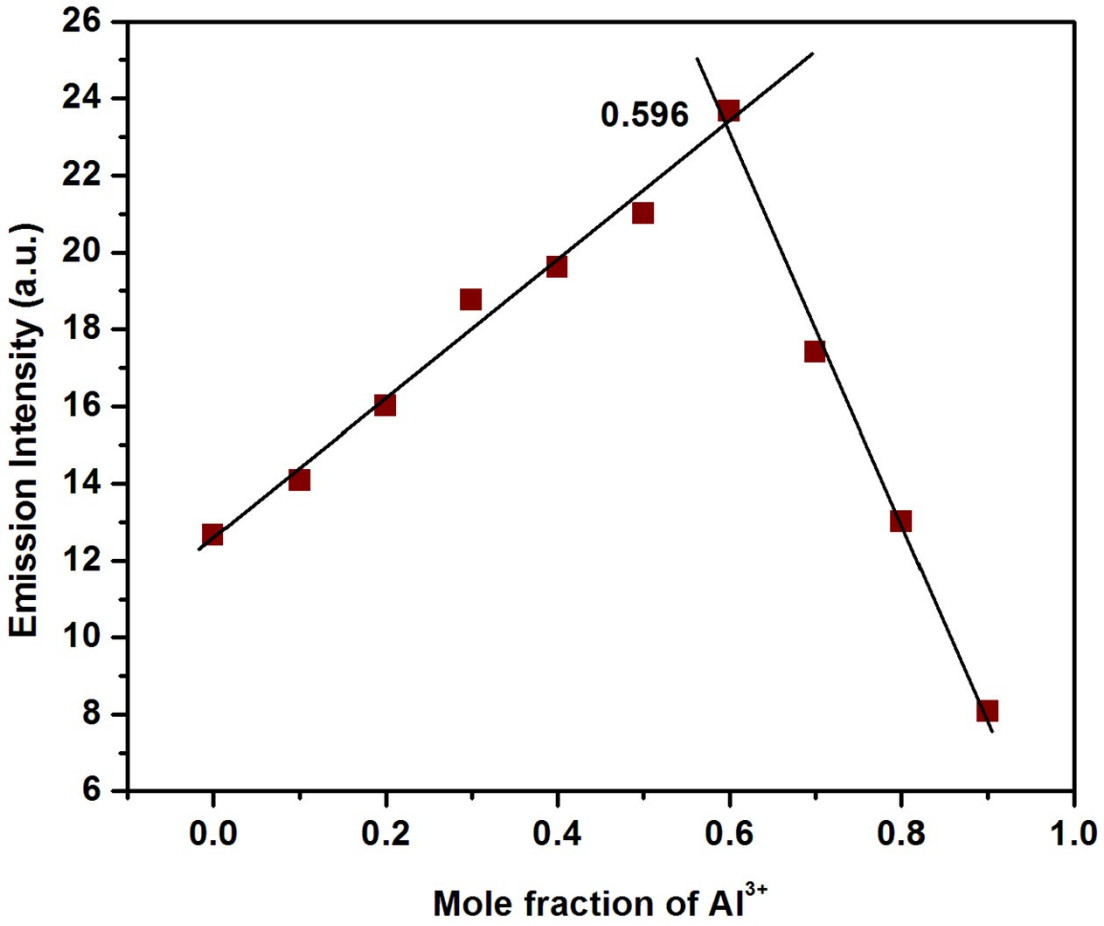

Fig. S12 Job's plot of the chemosensor HL for Al^{3+}.

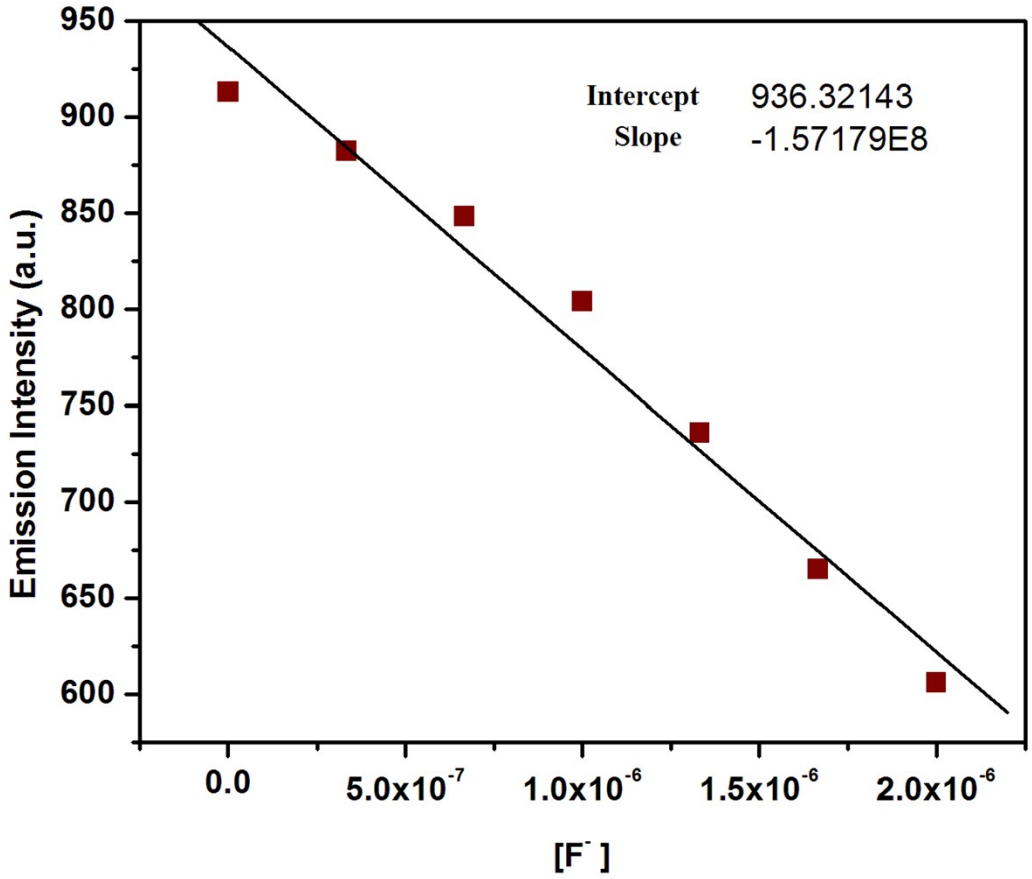

Fig. S13 Linear response curve of $[AlL_2]^+$ at 612 nm depending on the F^-concentration.

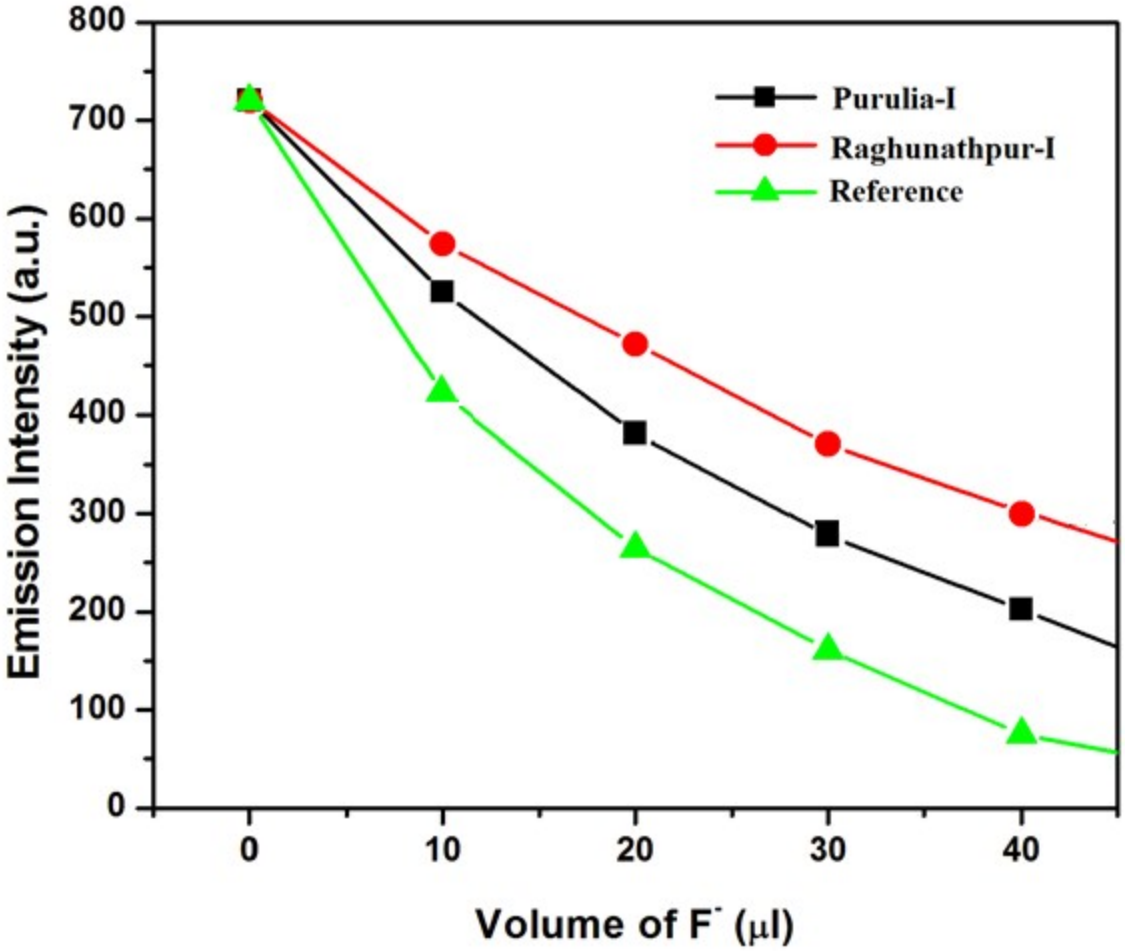

Fig. S14 Calibration plot between emission intensity of $[AlL_2]^+$ (Reference) at 612 nm vs volume of F^- for the analysis of F^- contamination in drinking water of Raghunathpur-I and Purulia-I in West Bengal.

Table S1 Some important bond length and bond angles of HL

Bond	**Length (Å)**
O(1) - C(1)	1.38
C(1) - C(2)	1.40
C(2) - N(1)	1.40
N(1) - N(2)	1.28

N(2) - C(3)	1.41
C(3) - C(4)	1.43
C(4) - N(3)	1.37

Bond	**Angle (°)**
O(1) - C(1) - C(2)	118.7
C(1) - C(2) - N(1)	112.98
C(2) - N(1) - N(2)	118.79
N(1) - N(2) - C(3)	114.69
N(2) - C(3) - C(4)	116.56
C(3) - C(4) - N(3)	119.81

Table S2 Some important bond length and bond angles of $[AlL_2]^+$

Bond	**Length (Å)**
N(1) - N(2)	1.31
N(2) - Al	1.94
Al- N(3)	2.00
N(3) - N(4)	1.28
O(1) - Al	1.88
O(2) - Al	1.86
N(5) - Al	1.99

N(6) - Al	2.08

Bond	**Angle (°)**
N(5) - Al - N(2)	81.94
N(2) - Al - O(2)	83.94
O(2) - Al- N(3)	87.31
N(3) - Al - N(6)	81.01
N(6) - Al – O(1)	92.52
O(1) - Al- N(5)	97.86

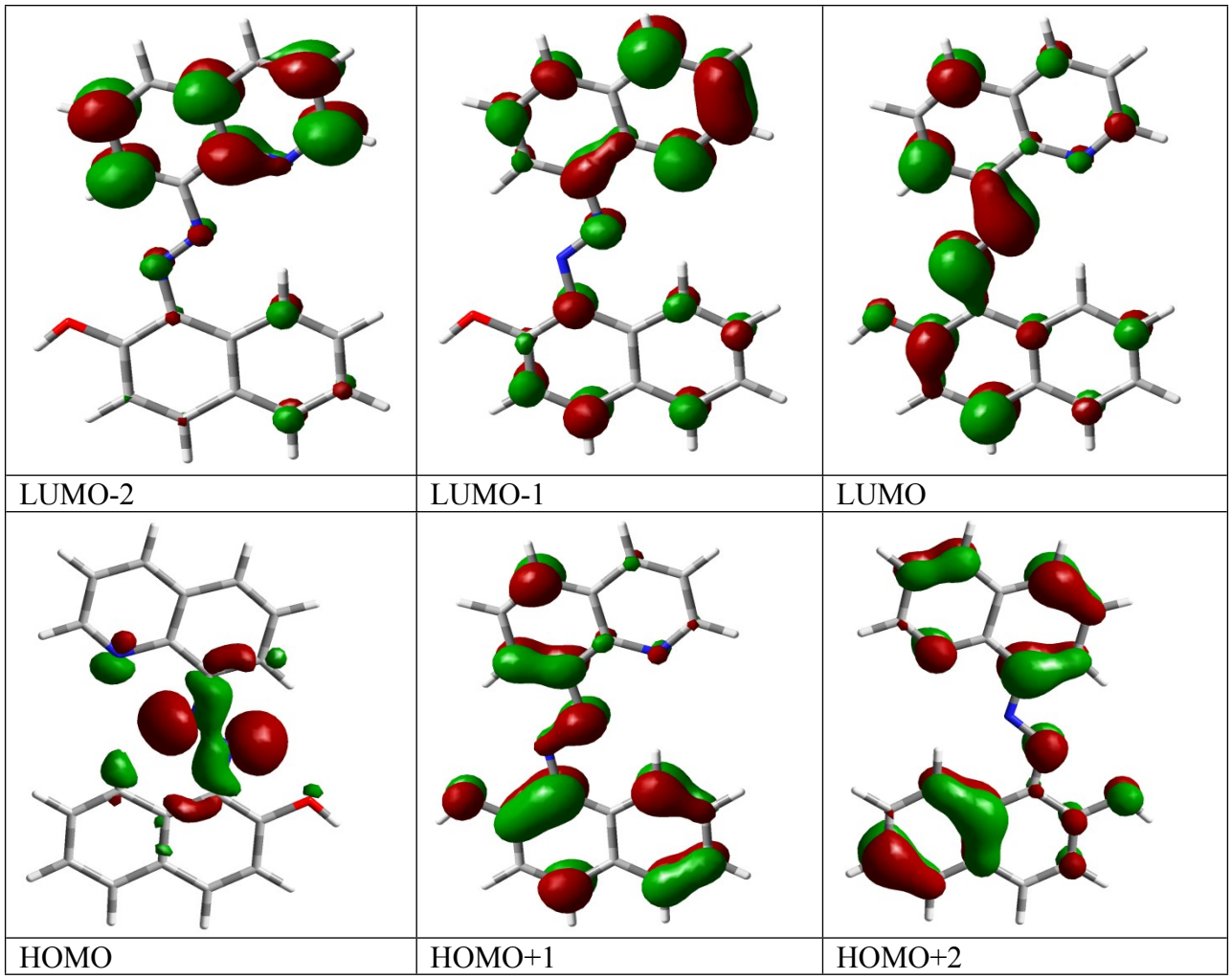

Fig. S15 Contour plots of some selected molecular orbitals of HL.

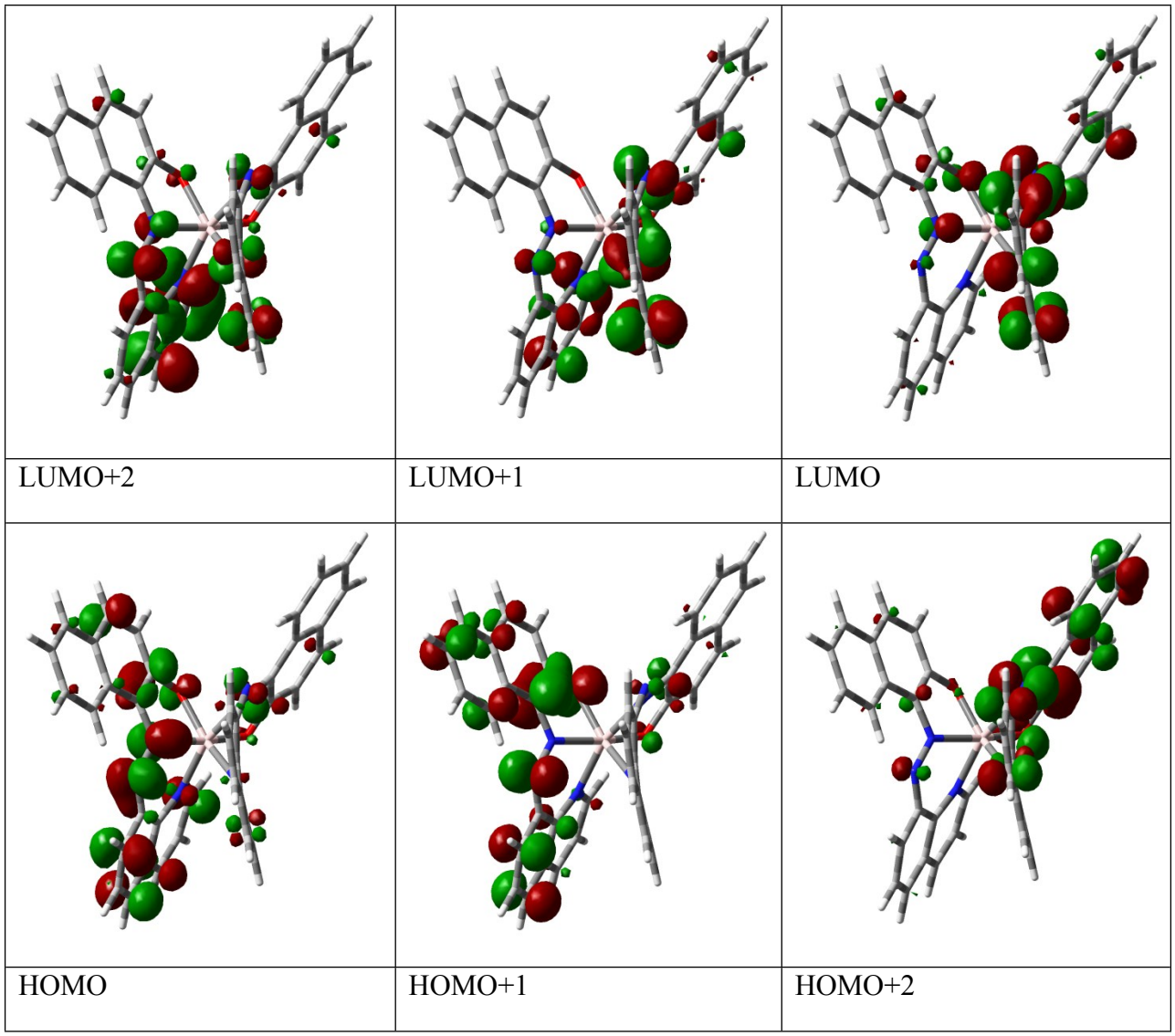

Fig. S16 Contour plots of some selected molecular orbitals of $[AlL_2]^+$ complex.

Table S3 MO composition of HL.

MO	**Energy (eV)**	**Naphthol**	**Quinoline**	**Azo**
LUMO+10	2.65	00	100	00
LUMO+9	2.65	18	79	03
LUMO+8	2.57	98	02	00
LUMO+7	1.5	52	31	17
LUMO+6	1.49	100	00	00
LUMO+5	1.06	43	53	04

LUMO+4	-0.02	99	01	00
LUMO+3	-0.25	47	39	14
LUMO+2	-0.38	11	85	04
LUMO+1	-1.17	27	69	04
LUMO	-2.31	34	33	33
HOMO	-5.31	11	13	76
HOMO-1	-5.43	63	27	10
HOMO-2	-6.36	50	44	06
HOMO-3	-6.43	89	10	01
HOMO-4	-6.61	02	94	04
HOMO-5	-6.91	00	100	00
HOMO-6	-7.43	63	28	09
HOMO-7	-8.36	30	66	04
HOMO-8	-8.41	87	12	01
HOMO-9	-9.01	88	03	09
HOMO-10	-9.22	05	90	05

Table S4 MO composition of $[AlL_2]^+$

MO	**Energy (eV)**	**Al**	**Ligands(HL)**
LUMO+10	0.48	01	99
LUMO+9	0.22	00	100
LUMO+8	0.11	02	98
LUMO+7	-0.13	01	99
LUMO+6	-0.53	00	100
LUMO+5	-0.78	00	100
LUMO+4	-0.85	00	100
LUMO+3	-1.22	00	100
LUMO+2	-2.01	00	100
LUMO+1	-2.21	01	99
LUMO	-3.06	01	99
HOMO	-3.87	01	99
HOMO-1	-5.08	00	100
HOMO-2	-5.5	00	100
HOMO-3	-5.87	00	100
HOMO-4	-6.12	02	98
HOMO-5	-6.27	00	100
HOMO-6	-6.45	01	99
HOMO-7	-6.85	01	99
HOMO-8	-7.07	01	99
HOMO-9	-7.33	00	100
HOMO-10	-7.48	00	100

Table S5 Vertical electronic transitions calculated by TDDFT/B3LYP/CPCM method for HL and $[AlL_2]^+$.

	Excitation energy (eV)	**Wavelength (nm)**	**Oscillation frequency(f)**	**Key Transitions**	**Nature of transitions**
HL	2.7869	528	0.7206	(99%) HOMO→LUMO	ILCT
$[AlL_2]^+$	2.2142	559.94	0.1193	(37%) HOMO→LUMO+5	ILCT